

## BARRIER HEIGHT DISTRIBUTIONS — THE INFLUENCE OF WEAK CHANNELS\*

A. TRZCIŃSKA<sup>a</sup>, E. PIASECKI<sup>a,b</sup>, W. CZARNACKI<sup>b</sup>, P. DECOWSKI<sup>c</sup>  
 N. KEELEY<sup>b</sup>, M. KISIELIŃSKI<sup>a,b</sup>, S. KLICZEWSKI<sup>d</sup>, P. KOCZON<sup>e</sup>  
 A. KORDYASZ<sup>a</sup>, M. KOWALCZYK<sup>a,f</sup>, S. KHLEBNIKOV<sup>g</sup>, E. KOSHCHIY<sup>h</sup>  
 T. KROGULSKI<sup>i</sup>, B. LOMMEL<sup>e</sup>, T. LOKTEV<sup>j</sup>, M. MUTTERER<sup>k</sup>  
 K. PIASECKI<sup>f</sup>, I. STROJEK<sup>b</sup>, W.H. TRZASKA<sup>l</sup>, S. SMIRNOV<sup>j</sup>  
 A. STOLARZ<sup>a</sup>, G. TIOURIN<sup>l</sup>

<sup>a</sup>Heavy Ion Laboratory, University of Warsaw, Warszawa, Poland

<sup>b</sup>National Centre for Nuclear Research, Świerk, Poland

<sup>c</sup>Smith College, Northampton, USA

<sup>d</sup>The Henryk Niewodniczański Institute of Nuclear Physics PAN, Kraków, Poland

<sup>e</sup>GSI Helmholtzzentrum für Schwerionenforschung GmbH, Darmstadt, Germany

<sup>f</sup>Institute of Experimental Physics, Warsaw University, Warszawa, Poland

<sup>g</sup>Khoplin Radium Institute, St. Petersburg, Russia

<sup>h</sup>Kharkiv University, Kharkiv, Ukraine

<sup>i</sup>Faculty of Physics, University of Białystok, Białystok, Poland

<sup>j</sup>JINR, Dubna, Russia

<sup>k</sup>Institute für Kernphysik, Technische Universität, Darmstadt, Germany

<sup>l</sup>University of Jyväskylä, Jyväskylä, Finland

*(Received November 26, 2013)*

We present a review of barrier height distribution studies performed at the Heavy Ion Laboratory (HIL) of the Warsaw University using  $^{20}\text{Ne}$  beams. The barrier height distributions for the  $^{20}\text{Ne}+^{58,60,61}\text{Ni}$ ,  $^{90,92}\text{Zr}$ ,  $^{118}\text{Sn}$  and  $^{208}\text{Pb}$  systems were experimentally determined. In some cases, a discrepancy between experimental results and the predictions of Coupled-Channels (CC) calculations was observed. We suggest that this discrepancy could be due to the cumulative effect of many individually weak channels, such as non-collective excitations of the target or transfer reactions, which cannot be implemented fully in practical CC or CRC calculations of standard form.

DOI:10.5506/APhysPolB.45.383

PACS numbers: 25.70.Bc, 25.70.Hi, 24.10.Eq

---

\* Presented at the XXXIII Mazurian Lakes Conference on Physics, Piaski, Poland, September 1–7, 2013.

## 1. Introduction

The basic reaction mechanism can be described in terms of a central potential which depends on the distance between the centers of mass of the target and projectile. At some distance, the potential has its maximum value, which is referred to as the Coulomb barrier. It arises due to the competition between the long-range repulsive Coulomb force and the short-ranged attractive nuclear force. A fusion event requires that the two interacting nuclei overcome or penetrate through the barrier. As near-barrier fusion is influenced by the intrinsic degrees of freedom of the interacting nuclei, the single barrier is split into many barriers due to various reaction channel couplings. It has been demonstrated experimentally in many systems that the fusion barrier between two nuclei does not have a unique value but rather a weighted distribution of heights,  $D_{\text{fus}}$ . Measurements of barrier height distributions are a long-term project of our group. The best theoretical description of this observable can be made within the Coupled-Channels (CC) method where the interplay between various reaction channels is taken into account.

## 2. The experimental method of barrier height distribution determination

$D_{\text{fus}}$  can be determined directly from fusion excitation function measurements [1] through the relation

$$D_{\text{fus}} = \frac{d^2(E\sigma)}{dE^2}, \quad (1)$$

where  $\sigma$  is the fusion cross section and  $E$  the incident energy.

Fusion measurements are rather difficult and require complicated experimental set-ups. There is also an alternative method to measure the barrier height distribution: it has been shown both theoretically and experimentally that the fusion measurements can be replaced by much simpler quasi-elastic (the sum of elastic, inelastic and transfers) scattering measurements at backward angles, giving rise to the barrier height distribution  $D_{\text{qe}}$ . It has been shown [2] that one can experimentally determine the barrier distribution from the flux of ions which have not penetrated the barrier. The cross section for quasi-elastic scattering,  $\sigma_{\text{qe}}$ , measured at backward angles, normalized to the cross section for Rutherford scattering,  $\sigma_{\text{Ruth}}$ , gives the barrier distribution via the following formula

$$D_{\text{qe}} = -\frac{d}{dE} \left( \frac{\sigma_{\text{qe}}}{\sigma_{\text{Ruth}}} \right). \quad (2)$$

Studies of barrier height distributions show that the structure of the interacting nuclei is reflected in the shape of the distribution. The best theoretical description of this phenomenon can be made within the Coupled-Channels (CC) method where the interplay between various reaction channels is taken into account. In some cases, one observes significant structure in a distribution, a “fingerprint” of the couplings involved [3, 4].

Usually, in CC calculations only strong collective excitations are taken into account. However, in some systems, there are many weak, non-collective excitations, the cumulative effect of which can be important. Including such excitations explicitly in a standard CC calculation is a practical impossibility due to the large number of channels involved, plus the detailed nature of the couplings — coupling strength and form factor — is usually not known. The influence of individual transfer couplings on the backward angle quasi-elastic scattering cross section is also usually weak, but, again, cumulatively such couplings may play an important role. However, while single-nucleon and  $\alpha$ -cluster transfers are easily implemented via coupled reaction channels (CRC) codes such as FRESKO [5], the number of channels necessary for a complete calculation can become impractical, particularly when multiple exit partitions are involved. The situation is further complicated for multi-step transfer paths where many of the required spectroscopic amplitudes are not known. Thus, proving the cumulative importance of the influence of many weak channels on the barrier distribution by explicit calculation within the standard CC or CRC formalism remains a practical impossibility for the present, although schematic models have been evolved that successfully demonstrate this, see *e.g.* Ref. [6].

### 3. Experimental results and discussion

The experimental program of our group is dedicated to  $^{20}\text{Ne}$  beams. The  $^{20}\text{Ne}$  nucleus has large deformation parameters:  $\beta_2 = 0.46$ ,  $\beta_3 = 0.39$ ,  $\beta_4 = 0.27$  [7–9]. Due to this significant deformation, in most cases the Ne structure should dominate the barrier distribution. CC calculations predict a barrier height distribution with two clearly seen maxima reflecting the structure of  $^{20}\text{Ne}$  projectile in scattering with medium or heavy target. The back-scattering method of  $D_{\text{qe}}$  was employed to determine the barrier distributions. Measurements were performed at HIL using a  $^{20}\text{Ne}$  beam from the Warsaw Cyclotron. We used a compact (40 cm diameter) scattering chamber equipped with 30  $1\text{ cm} \times 1\text{ cm}$  detectors placed at backward angles (130, 140 and 150 degrees) measuring energy of quasi-elastically scattered ions. Two detectors placed at forward angles (35 degrees) measured the Rutherford scattering and were also used to calibrate the beam energy.

As the excitation function depends on the angle (due to the centrifugal potential), all measurement were transformed to the reference angle of 180 degrees using an effective energy,  $E_{\text{eff}}$ , given as

$$E_{\text{eff}} = \frac{2E}{1 + \text{cosec}(\theta/2)}, \quad (3)$$

where  $E$  is the beam energy and  $\theta$  is the scattering angle in the c.m.s.

In Fig. 1, a compilation of barrier height distributions measured for  $^{20}\text{Ne}$  interacting with  $^{\text{nat}}\text{Ni}$ ,  $^{90,92}\text{Zr}$ ,  $^{118}\text{Sn}$ ,  $^{208}\text{Pb}$  is shown [10–12]. For  $^{208}\text{Pb}$ , the barrier distribution was measured not only using the back-scattering method but also with the fusion method. The predictions of CC calculations (performed with CCQEL code [13]) are also plotted: for all systems studied, the theoretical model predicts barrier distribution with two maxima. The experimental data show such a structure only for the  $^{90}\text{Zr}$  and  $^{\text{nat}}\text{Ni}$  cases. For all other nuclei, the experimental barrier distributions are smooth and do not reveal any structure.

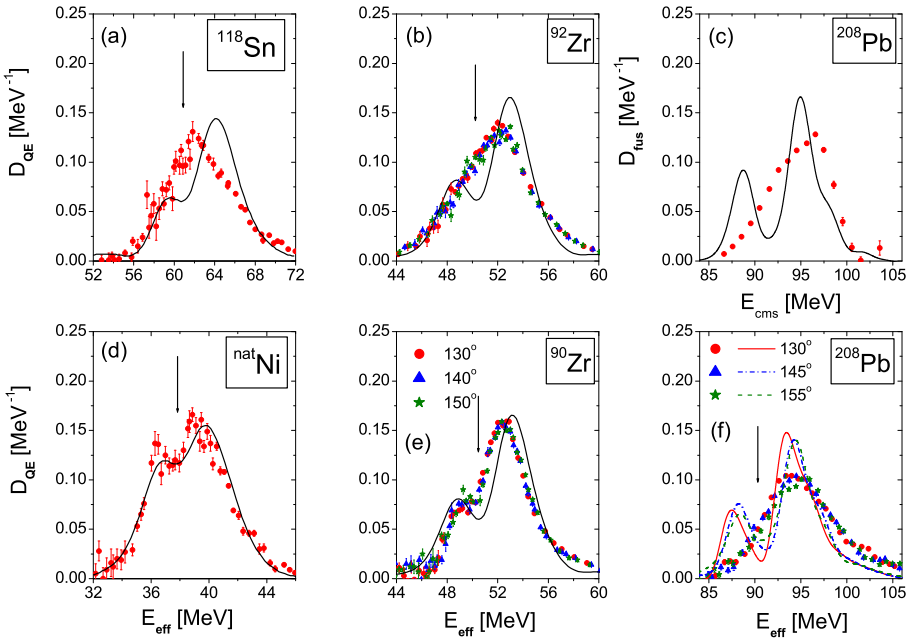


Fig. 1. Barrier height distributions for  $^{20}\text{Ne}$  interacting with  $^{\text{nat}}\text{Ni}$ ,  $^{90,92}\text{Zr}$ ,  $^{208}\text{Pb}$  nuclei (for the  $^{208}\text{Pb}$  target  $D_{\text{fus}}$  and  $D_{\text{eq}}$  distributions are shown in the panels (c) and (f), respectively). Experimental data are plotted as points — different symbols denote different measurement angles in the laboratory frame. The curves denote the results of CC calculations folded with the experimental energy resolution.

One should stress that according to standard CC calculations, the barrier distributions for  $^{90}\text{Zr}$  and  $^{92}\text{Zr}$  targets should be practically indistinguishable, being completely dominated by the strong  $^{20}\text{Ne}$  deformation.

The suggested reason for the discrepancy between experiment and theoretical predictions was the effect of transfer reaction channels as they were not taken into account in the basic CC calculations.

To check this hypothesis, transfer cross sections were also measured for the systems discussed above at energies corresponding to the predicted or observed minima in the barrier distributions.

The masses of transfer reaction products were identified with the ToF method, whereas their atomic numbers were determined using a  $\Delta E-E$  telescope. A multi-channel plate detector for the “start” and four silicon PIN diode type detectors giving a “stop” signal were placed at backward angle ( $142^\circ$ ). The telescope was placed at  $142^\circ$  (symmetrically in respect to beam axis). The flight-path of the system was 82 cm.

In Fig. 2, the results of the measurements are presented. The total transfer cross section for  $^{208}\text{Pb}$  is quite substantial and one might suspect that in this case the transfer channels are responsible for smoothing out the predicted structure in the barrier height distribution. However, for  $^{90}\text{Zr}$  and  $^{92}\text{Zr}$  the total cross sections for all transfer channels are much smaller and are similar for both isotopes. Thus, one cannot explain the differences between the observed barrier distribution for the systems:  $^{20}\text{Ne}+^{90}\text{Zr}$  and  $^{20}\text{Ne}+^{92}\text{Zr}$  by transfers.

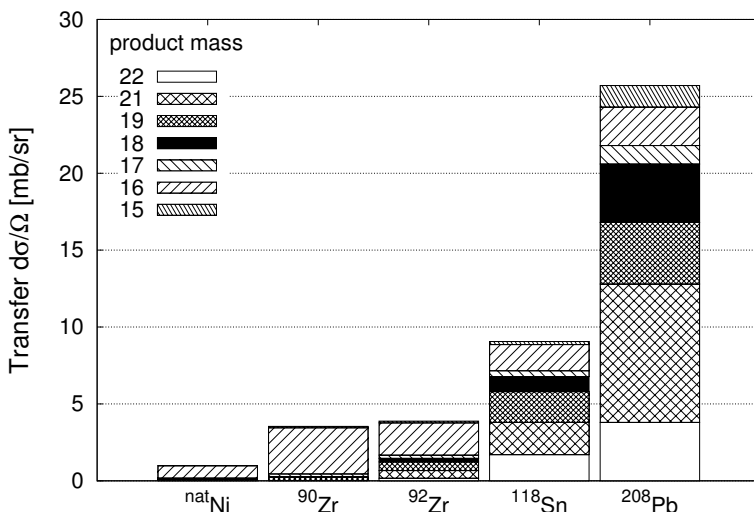


Fig. 2. Transfer channel differential cross sections at  $142.5^\circ$  for  $^{20}\text{Ne}$  and various targets at energies close to the barrier.

These two Zr isotopes differ in their level densities:  $^{90}\text{Zr}$  as a semi-magic nucleus has much lower level density. The heavier  $^{92}\text{Zr}$  has two valence neutrons outside the  $N = 50$  shell and due to this its level density is significantly higher.

It was noticed in the excitation energy ( $Q$ -value) spectra of both systems that for  $^{92}\text{Zr}$  in the energy region above 5 MeV there are more events than for  $^{90}\text{Zr}$ . In this energy region, collective excitations are negligible. This could be evidence that there are more single particle excitation for  $^{92}\text{Zr}$  than for  $^{90}\text{Zr}$  and one can try to explain the smoothing out of the structure in barrier height distribution for  $^{92}\text{Zr}$  due to this phenomenon.

In order to test this hypothesis, barrier distributions for three Ni isotopes were studied:  $^{58}\text{Ni}$ ,  $^{60}\text{Ni}$  and  $^{61}\text{Ni}$  [14] which differ in their level densities (see Fig. 3).  $^{58}\text{Ni}$  as a semi-magic nucleus has a relatively low level density, whereas  $^{61}\text{Ni}$  has a much higher level density and for  $^{60}\text{Ni}$  the situation is in-between.

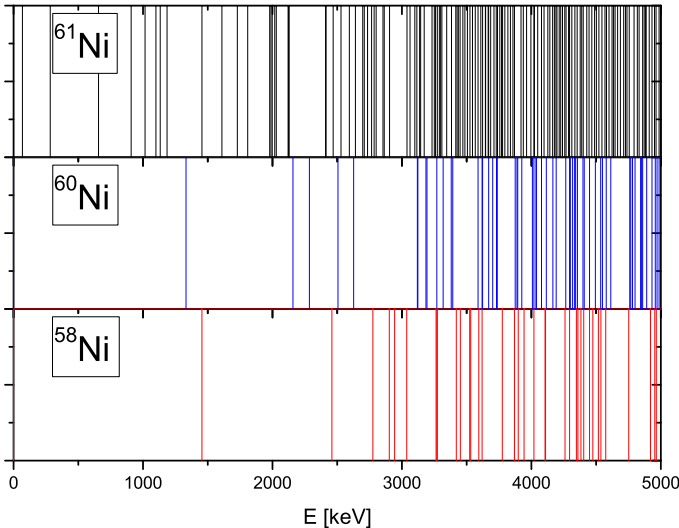


Fig. 3. Adopted experimental levels in  $^{58,60,61}\text{Ni}$  (from [www.nndc.bnl.gov/nudat2](http://www.nndc.bnl.gov/nudat2)).

Results of the measurements are presented in Fig. 4. As expected, for  $^{58}\text{Ni}$ , where single-particle excitations should not be numerous, there is a clearly seen structure (two maxima) in the barrier distribution. For  $^{60}\text{Ni}$ , the structure is less marked whereas for  $^{61}\text{Ni}$ , where the level density is the highest, the structure at 37 MeV is completely smoothed out. The energy resolution for all cases was the same:  $\text{FWHM} \approx 0.8$  MeV.

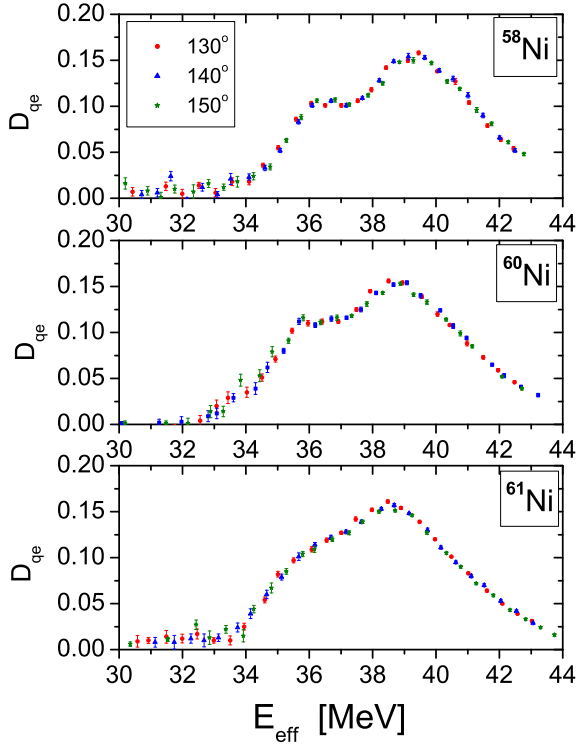


Fig. 4. Barrier height distributions for the  $^{20}\text{Ne}+^{58,60,61}\text{Ni}$  systems.

The transfer cross sections for these three systems:  $^{20}\text{Ne}+^{58,60,61}\text{Ni}$  were also measured: they are similar for all 3 isotopes ( $\simeq 1$  mb/sr) [15].

#### 4. Discussion and conclusions

The barrier distribution was experimentally determined for several systems:  $^{20}\text{Ne} + ^{58,60,61}\text{Ni}$ ,  $^{90,92}\text{Zr}$ ,  $^{118}\text{Sn}$  and  $^{208}\text{Pb}$ . Contrary to model predictions based on Coupled-Channels calculations, in many cases the experimental barrier height distributions do not reveal any structure. Only for  $^{58}\text{Ni}$ ,  $^{90}\text{Zr}$  and partially for  $^{60}\text{Ni}$  were the two maxima predicted by theory observed.

We suggest that the discrepancy between the calculations and experiment can be caused by the effect of weak reaction channels like transfers or single particle excitations neglected in standard calculations. Only strong reaction channels — collective excitations — were taken into account in these calculations.

In  $^{61}\text{Ni}$  and  $^{92}\text{Zr}$ , most probably the single particle excitations are responsible for smoothing out the predicted structure in the barrier distributions: for both isotopes the transfer cross sections in the interaction with  $^{20}\text{Ne}$  at near-barrier energies are low whereas they both have high level densities.

In  $^{208}\text{Pb}$ , rather the various transfer channels caused the lack of structure in the barrier distribution as the cross section for these processes is quite substantial and  $^{208}\text{Pb}$  as a doubly-magic nucleus has low level density.

For  $^{118}\text{Sn}$ , probably both effects have an influence on the barrier distribution shape as for  $^{20}\text{Ni}+^{118}\text{Sn}$  the transfer cross sections as well as the level density are relatively high.

## REFERENCES

- [1] N. Rowley *et al.*, *Phys. Lett.* **B254**, 25 (1991).
- [2] H. Timmers *et al.*, *Nucl. Phys.* **A584**, 190 (1995).
- [3] M. Dasgupta *et al.*, *Annu. Rev. Nucl. Part. Sci.* **48**, 401 (1998).
- [4] A.M. Stefanini *et al.*, *Phys. Rev. Lett.* **74**, 864 (1995).
- [5] I.J. Thompson, *Comput. Phys. Rep.* **7**, 167 (1988).
- [6] S. Yusa, K. Hagino, N. Rowley, *Phys. Rev.* **C82**, 024606 (2010).
- [7] S. Raman *et al.*, *At. Data Nucl. Data Tables* **78**, 1 (2001).
- [8] R.H. Spear, *At. Data Nucl. Data Tables* **42**, 55 (1989).
- [9] G. Blanpied *et al.*, *Phys. Rev.* **C38**, 2180 (1988).
- [10] E. Piasecki *et al.*, *Phys. Rev.* **C80**, 054613 (2009).
- [11] E. Piasecki *et al.*, *Phys. Rev.* **C85**, 054604 (2012).
- [12] E. Piasecki *et al.*, *Phys. Rev.* **C85**, 054608 (2012).
- [13] K. Hagino, N. Rowley, unpublished.
- [14] A. Trzcińska, presented at FUSION11 conference, May 2013, St. Malo, France.
- [15] A. Trzcińska, to be published.